

Electrode Kinetics of Metal Complexes Confined in Perfluoro Polycarboxylate and Polysulfonate Coatings on Graphite Electrodes

Noboru OYAMA,* Takeo OHSAKA, Tooru USHIROGOUCHI, Sachiko SANPEI,†
and Sadako NAKAMURA†

Department of Applied Chemistry for Resources, Tokyo University of Agriculture and Technology,
Koganei, Tokyo 184

†Department of Chemistry, Japan Women's University, Mejirodai, Bunkyo-ku, Tokyo 112

(Received December 2, 1987)

A heterogeneous electron-transfer process of $[\text{Os}(\text{bpy})_3]^{2+/3+}$ (bpy: 2,2'-bipyridine) and [(trimethylammonio)methyl]ferrocene/ferricinium ($\text{TAF}^{+/2+}$) redox couples, which were confined in perfluoro polycarboxylate and polysulfonate polyelectrolyte coatings on graphite electrodes, at the electrode/film interfaces as well as a homogeneous charge-transport process within the coating films were examined by means of potential-step chronoamperometry and chronocoulometry, normal pulse voltammetry and ac impedance measurements. The relevant kinetic parameters (i.e., the standard rate constant k^0 and the transfer coefficient of the heterogeneous electron-transfer process and the apparent diffusion coefficient D_{app} for the homogeneous charge-transport process) were determined at various concentrations of the redox species in the films at various pH's. The temperature dependences of D_{app} , k^0 and the formal potentials of the $[\text{Os}(\text{bpy})_3]^{2+/3+}$ and $\text{TAF}^{+/2+}$ couples confined in the films were also examined and the relevant activation parameters for the heterogeneous electron-transfer and homogeneous charge-transport processes and the reaction entropies of these redox couples were evaluated. On the basis of the kinetic and thermodynamic data obtained, the mechanism of the charge-transport process within the films, the effects of polymer domain and pH on the rates of the heterogeneous electron-transfer and homogeneous charge-transport processes and on the incorporation of the redox species into the films, etc. are discussed.

Recently, much attention has been denoted to the electron-transfer processes at electroactive, thin polymer film-coated electrodes from the viewpoint of the fundamental studies on the mechanism and kinetics of electron transfer as well as the possible applications based on their interesting properties (e.g., electron-transfer catalysis (and mediation), redox conductivity and electrochromic property).¹⁾ We have also been interested in this problem and have continued to conduct the kinetic and thermodynamic study of (i) the heterogeneous electron-transfer process between electrode and redox species (or sites) confined in polymeric domains and (ii) the homogeneous charge-transport process within polymer coatings for various types of redox polymer-coated electrode systems.^{2–14)} They involve (1) multiply-charged anionic metal complexes-electroinactive cationic polyelectrolyte film systems^{2,4,7,8,11,13)} (e.g., $[\text{Mo}(\text{CN})_8]^{4-/3-}$, $[\text{Fe}(\text{CN})_6]^{4-/3-}$, $[\text{W}(\text{CN})_8]^{4-/3-}$ and $[\text{IrCl}_6]^{3-/2-}$ -protonated poly(4-vinylpyridine) (PVP) systems and $[\text{Fe}(\text{CN})_6]^{4-/3-}$, $[\text{Mo}(\text{CN})_8]^{4-/3-}$, $[\text{Fe}(\text{bp})_3]^{4-/3-}$ (bp: bathophenanthroline disulfonate) and $[\text{W}(\text{CN})_8]^{4-/3-}$ -electropolymerized poly(*N,N*-dialkylaniline) film systems), (2) polymer ligand-containing metal complex systems²⁾ (e.g., $[\text{Fe}(\text{CN})_5]^{3-/2-}$ -PVP system), (3) viologen polymer film systems^{5,6,9)} (e.g., *N,N'*-dimethyl-4,4'-bipyridinium-Nafion system, poly(xylylviologen) (PXV)-poly(*p*-styrenesulfonate) (PSS) system, poly(styrene-*co*-chloromethylstyrene) pendant viologen (PMV) film systems, and PMV-Nafion and -PSS systems) and (4) electropolymerized electroactive film systems^{10,12,14)} (e.g., poly(1-pyrenamine) and poly(*o*-phenylenediamine) film systems).

In the present report, we will describe the kinetic study concerning the electrode reactions ((i) and (ii)) of cationic redox couples (i.e., $[\text{Os}(\text{bpy})_3]^{2+/3+}$ (bpy: 2,2'-bipyridine) and [(trimethylammonio)methyl]ferrocene/ferricinium ($\text{TAF}^{+/2+}$))-containing perfluoro polycarboxylate and polysulfonate polyelectrolyte coatings (Fig. 1) on graphite electrodes by means of potential-step chronoamperometry and chronocoulometry, normal pulse voltammetry and ac impedance measurements. Previously, Bard et al.¹⁵⁾ have examined the mechanism of charge transport through Nafion polymers (coated on glassy carbon electrodes)

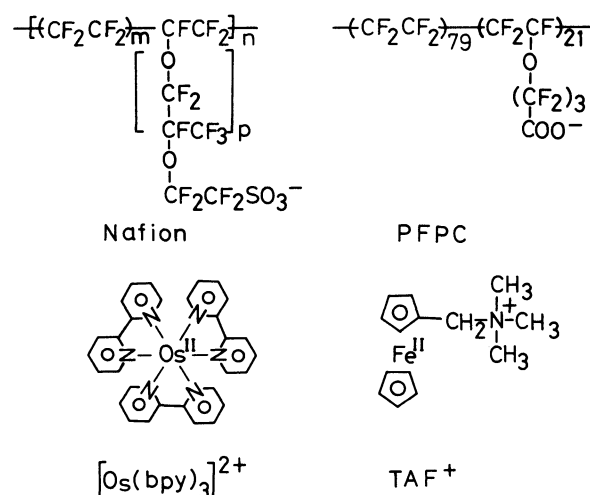


Fig. 1. Structures of the perfluoro polycarboxylate (PFPC) and polysulfonate (Nafion) polyelectrolytes, $[\text{Os}(\text{bpy})_3]^{2+}$ and [(trimethylammonio)methyl]ferrocene (TAF^{+}) used in this study.

containing some redox species such as $[\text{Os}(\text{bpy})_3]^{2+}$ and TAF^+ on the basis of the estimation of the apparent diffusion coefficient (D_{app}) for the charge-transport process within the films containing these redox species and the diffusion coefficients of actual mass transport of the same redox species through the polymer. Also, Anson et al.¹⁶ have reported the shifts in formal redox potentials accompanying the incorporation of cationic complexes (including $[\text{Os}(\text{bpy})_3]^{2+}$ and TAF^+) in perfluoro polycarboxylate and polysulfonate coatings on graphite electrodes. Our aim is to elucidate and understand the effect of polymer domain on the rates of both heterogeneous electron-transfer process and homogeneous charge-transport process and the dependences of the standard rate constant (k°) for the former process and the apparent diffusion coefficient (D_{app}) for the latter process upon concentration of redox species confined in the polymeric coatings. The temperature dependences of the formal redox potentials of the $[\text{Os}(\text{bpy})_3]^{2+/3+}$ and $\text{TAF}^{+/2+}$ couples confined in the coatings, k° and D_{app} will be also examined in order to gain an additional insight into some possible factors controlling the rates of the heterogeneous electron-transfer and homogeneous charge-transport processes.

Experimental

Materials. Nafion membrane 125®, which is a perfluoro polysulfonate polyelectrolyte membrane, was obtained from E.I. du Pont de Nemours and Company (Wilmington, Delaware). According to a previous procedure,^{5,6,17} the stock solution of Nafion was prepared from the membrane in order to facilitate the electrode coating. Then, an ethanol-dimethyl sulfoxide (EtOH-DMSO) mixture (50:50 volume percent) was used as a solvent and the concentration of Nafion was 3.6 mg ml^{-1} . Nafion coating films were prepared by evaporation of aliquots of the stock solution put on electrode surfaces. Perfluoro polycarboxylate polyelectrolyte (abbreviated as PFPC in this paper and shown in Fig. 1 together with Nafion) was obtained in the form of a fine suspension of the methyl ester from Asahi Glass Company (Tokyo). The suspension (15 mg) was dissolved in EtOH-DMSO (50:50 volume percent) mixture solution. The concentration of the prepared stock solution of PFPC (as the methyl ester form) was 3.6 mg ml^{-1} . To prepare the coating films on electrodes, aliquots ($1\text{--}10 \mu\text{l}$) of the stock solution were evaporated on freshly cleaved electrodes. The resulting deposit was exposed to 1 M ($1 \text{ M} = 1 \text{ mol dm}^{-3}$) NaOH solution for 5 min to hydrolyze the ester to the carboxylate, and the electrode was then washed thoroughly with water. From the measurement of IR spectra of the PFPC film deposited on a glass slide, which was treated as mentioned above, it was confirmed that the extent of the hydrolysis under such a treatment is almost 100%.

$[\text{Os}(\text{bpy})_3](\text{ClO}_4)_2$ (bpy: 2,2'-bipyridine) was synthesized according to the standard procedure.¹⁸ [(Trimethylammonio)methyl] ferrocene bromide (abbreviated as TAF^+Br^- , see Fig. 1) was reagent grade (Tokyo Kasei Co.) and was used as received. The basal-plane pyrolytic graphite (BPG)

(Union Carbide Co.) disk electrodes (area: 0.17 cm^2) were prepared and mounted into glass tube with heat-shrinkable polyolefin tube as previously described.¹⁹ Aqueous solutions were prepared from doubly distilled water. The supporting electrolyte solution was 0.2 M CF_3COONa (Aldrich) adjust to pH 1.0, 2.0, and 3.0 with CF_3COOH and to pH 4.0 and 5.5 with 0.1 M $\text{CH}_3\text{COONa}\text{--CH}_3\text{COOH}$. Other chemicals were reagent grade and were used as received.

Apparatus and Procedures. A standard three-electrode electrochemical cell was used for all electrochemical experiments. The electrode assembly consisted of a film-coated BPG electrode as working electrode, a sodium chloride saturated calomel electrode (SSCE) as reference electrode and a spiral platinum as counter electrode. For cyclic voltammetry, potential-step chronoamperometry (and chronocoulometry), and normal pulse voltammetry, a home-made instrument was employed along with an X-Y recorder and a Nicolet digital oscilloscope (model 309).²⁻¹⁴ Positive feed-back circuitry was employed to compensate the resistances (these were typically ca. $20\text{--}50 \Omega$) associated with the polymer coatings as much as possible. Potential-step chronoamperometric (and chronocoulometric) data (i.e., current-time and charge-time responses) were stored in the digital oscilloscope and then transferred via an interface (NEC, RSC-232C) to a microcomputer (NEC, PC-9801E) where an analysis of the data was performed. In normal pulse voltammetric experiments, the pulse width of $10\text{--}100 \text{ ms}$ and the interval of $30\text{--}120 \text{ s}$ between successive pulses were employed. Thus it can be safely considered that the depletion layer of reactants produced during the preceding pulse completely disappears before the following pulse starts. Normal pulse voltammetric measurements were confined to times (typically $1\text{--}10 \text{ ms}$) sufficiently short to ensure that semi-infinite linear diffusion prevailed. The ac impedance measurements were performed with a Frequency Response Analyzer (Solartron Model 1250) and a Potentiostat/Galvanostat 2000 (Toho Technical Research, Tokyo) as previously described.⁷

The Nafion or PFPC film-coated electrodes were soaked in $0.1\text{--}5.0 \text{ mM}$ solutions (pH 1.0) (containing 0.2 M CF_3COONa) of metal complexes for $1\text{--}30 \text{ min}$ in order to achieve the incorporation of desired quantities of metal complexes into the films. After that, the electrodes were replaced in a pure supporting electrolytic solution (0.2 M CF_3COONa , pH 1.0) and then the cyclic voltammograms were recorded. After the steady-state cyclic voltammograms were obtained, the quantity (Γ_p) of metal complexes incorporated into the films deposited on electrodes was estimated (in mol cm^{-2}) by measuring the charge required in a potential-step experiment to quantitatively oxidize or reduce the metal complexes and/or measuring the area of cyclic voltammograms (for the oxidation-reduction reactions of the incorporated metal complexes) obtained at slow potential scan rates. The Γ_p values estimated by the two procedures were the same within experimental error. The molar concentrations (C_p^0 in mol cm^{-3}) of the incorporated metal complexes were calculated from the Γ_p 's thus obtained by using the thicknesses of the films which were estimated from their densities (mentioned below) under swelling state.

The film thicknesses under the "swelling" state were measured with a Surfcom 550 A (Surface Texture Measuring Instrument, Tokyo Seimitsu Co.). In this case, the samples

of wet Nafion films (thicknesses $>2 \times 10^{-5}$ cm) were produced by soaking the Pt-sputtered dry Nafion films coated on electrodes (the thickness of the Pt film coated $<1 \times 10^{-6}$ cm) in 0.2 M CF_3COONa solution (pH 1.0) for several hours and sorbing the water on the film surface by filter paper. The weight of the wet Nafion films (without Pt-sputtered films) coated on electrodes was also measured. The results indicated that the density of the wet Nafion film is $2.0 \pm 0.3 \text{ g cm}^{-3}$, which is in good agreement with the previously reported value.^{17,20} The wet thicknesses of the Nafion films incorporating various concentrations of the $[\text{Os}(\text{bpy})_3]^{2+}$ (or TAF^+) complex were independent of the concentration of the incorporated $[\text{Os}(\text{bpy})_3]^{2+}$ (or TAF^+) and were almost equal to those obtained for the swollen Nafion films containing no $[\text{Os}(\text{bpy})_3]^{2+}$ (or TAF^+). With the PFPC film, at first by soaking the PFPC film-coated electrodes in 1 M NaOH for several tens of minutes for the hydrolysis of the methyl ester in the films and then by following the procedure similar to that used in the estimation of the densities of the swollen Nafion films, the density of the wet PFPC film was estimated to be $2.0 \pm 0.4 \text{ g cm}^{-3}$, being independent of the incorporation of $[\text{Os}(\text{bpy})_3]^{2+}$ (or TAF^+).

The experiments concerning temperature dependences of the formal potentials (E^0), the apparent diffusion coefficients (D_{app}) for the diffusion-like charge-transport process within the films and the standard rate constant (k^0) of the heterogeneous electron-transfer reaction at the electrode/film interfaces were carried out in a "non-isothermal electrochemical cell"²¹⁻²⁴ having a thermally jacketed compartment for the working and counter electrodes and a separate compartment for the reference electrode which was connected to the cell with a 3 M NH_4Cl salt bridge. The reference electrode was maintained at a fixed temperature ($25 \pm 0.2^\circ\text{C}$). The temperature of the cell was varied in the range of $5-45^\circ\text{C}$. The values of E^0 were estimated as the average of the anodic and cathodic peak potentials of the cyclic voltammograms. The analysis of the data obtained was made according to the references²¹⁻²⁸ where the principles and assumption²¹⁻²⁴ involved in the use of such cells have been examined in detail and several recent

experimental examples of their successful applications are available.²⁵⁻²⁸

Nitrogen gas was passed through the solutions to remove the dissolved oxygen before the experiments and over the solution during the experiments. Potentials were measured and are reported with respect to an SSCE. Experiments were conducted at ambient laboratory temperature ($25 \pm 1^\circ\text{C}$), except for those concerning the temperature dependences of E^0 , D_{app} , and k^0 .

Results

Potential-Step Chronoamperometry and Chronocoulometry. Figure 2 shows the typical cyclic voltammograms for the $\text{TAF}^{+/2+}$ (or $[\text{Os}(\text{bpy})_3]^{2+/3+}$) couple confined in the PFPC film on BPG electrodes in 0.2 M CF_3COONa solution (pH 5.5). The wave

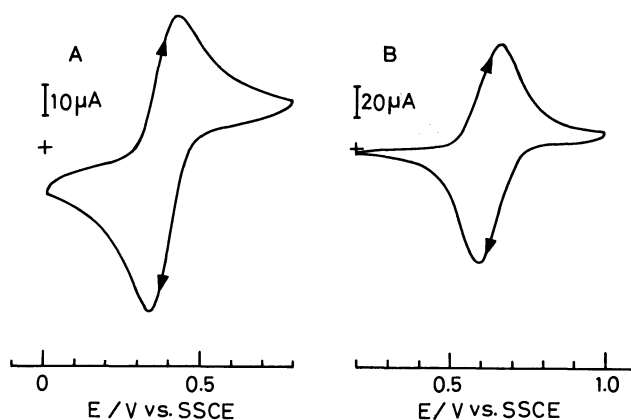


Fig. 2. Typical cyclic voltammograms for the redox reactions of (A) $\text{TAF}^{+/2+}$ and (B) $[\text{Os}(\text{bpy})_3]^{2+/3+}$ couples confined in the PFPC films on BPG electrodes in 0.2 M CF_3COONa solution (pH 5.5) containing 0.1 M $\text{CH}_3\text{COONa}/\text{CH}_3\text{COOH}$ buffer. Concentrations of redox species in the PFPC films (thickness: 2.1×10^{-5} cm): (A) 1.9×10^{-4} and (B) $2.3 \times 10^{-4} \text{ mol cm}^{-3}$. Scan rate: 200 mV s^{-1} .

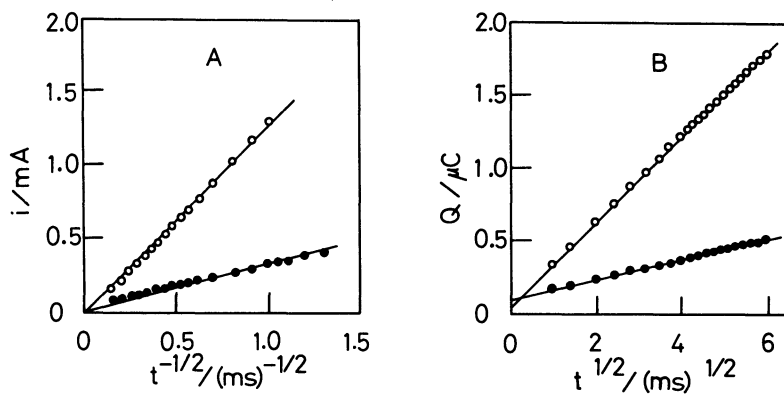


Fig. 3. Typical examples of the potential-step chronoamperometric and chronocoulometric Cottrell plots of (A) i vs. $t^{-1/2}$ and (B) Q vs. $t^{1/2}$ for the oxidation of the TAF^+ (●) and $[\text{Os}(\text{bpy})_3]^{2+}$ (○) complexes confined in the PFPC film on BPG electrodes. Other experimental conditions are the same as in Fig. 2.

shapes are similar to those for the solution-phase TAF^{+2+} (or $[\text{Os}(\text{bpy})_3]^{2+/3+}$) couple at a bare electrode, that is, the waves are diffusion-like, with broad peaks and diffusion tails. Typical examples of the potential-step chronoamperometric and chronocoulometric responses for the oxidation of the TAF^+ (or $[\text{Os}(\text{bpy})_3]^{2+}$) complex confined in the PFPC film are shown in Fig. 3. These i vs. $t^{-1/2}$ and Q vs. $t^{1/2}$ plots (i : current; Q : charge; t : time) are linear, indicating that the charge-transport processes within the films follow the Fick's diffusion laws.²⁻¹⁴ Thus, the slopes of these plots yielded the values of the apparent diffusion coefficients (D_{app}) for the diffusional charge transport. The D_{app} values obtained from these both plots were almost the same. The linear i vs. $t^{-1/2}$ and Q vs. $t^{1/2}$ plots were also obtained at various concentrations of the $[\text{Os}(\text{bpy})_3]^{2+}$ (or TAF^+) complex confined in the PFPC and Nafion films on electrodes in supporting electrolytic solutions of various pH's, and thus the relevant D_{app} 's were estimated from the slopes of these plots. The obtained data are summarized in Fig. 4.

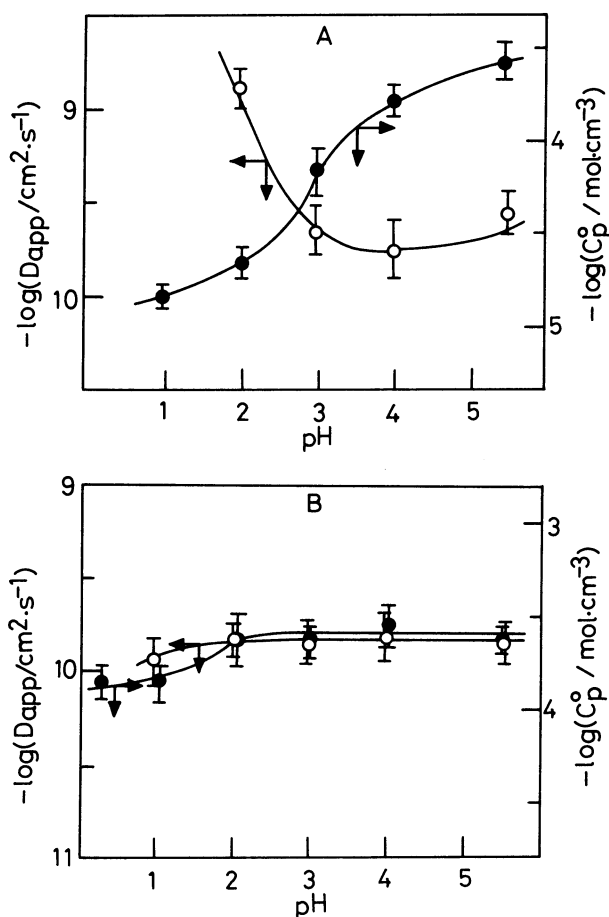


Fig. 4. pH dependences of C_p^0 and D_{app} for (A) $[\text{Os}(\text{bpy})_3]^{2+}$ -PFPC and (B) TAF^+ -PFPC systems. The amount of the PFPC coatings: $4.2 \times 10^{-5} \text{ g cm}^{-2}$. Supporting electrolyte: 0.2 M CF_3COONa . The values of D_{app} were estimated by potential-step chronoamperometry and chronocoulometry.

The D_{app} 's were found to depend on the incorporated redox species, their concentrations (C_p^0), the polymer films incorporating them, and the pH value of a solution.

Normal Pulse Voltammetry. Figure 5 shows the typical normal pulse voltammograms for the oxidation of the $[\text{Os}(\text{bpy})_3]^{2+}$ (or TAF^+) complex confined in Nafion films on BPG electrodes in 0.2 M CF_3COONa solution (pH 5.5) at various sampling times (τ). These S-shaped waves are similar to those obtained for solution-phase redox species at an uncoated electrode^{29,30} as well as for other redox compounds incorporated electrostatically into (or bound covalently to) polymer films on electrodes.^{2-6,8-14} The half-wave potentials of the voltammograms shifted to more positive values with decreasing τ . Plots of the anodic limiting current (i_{lim}) of these

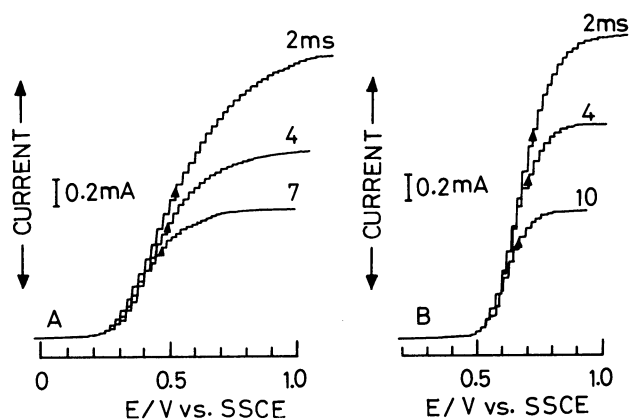


Fig. 5. Typical normal pulse voltammograms for the oxidation of (A) TAF^+ and (B) $[\text{Os}(\text{bpy})_3]^{2+}$ complexes confined in the Nafion films on BPG electrodes at various sampling times. Concentration of SO_3^- group in Nafion films: $1.65 \times 10^{-3} \text{ mol cm}^{-3}$. Film thickness: $4.3 \times 10^{-5} \text{ cm}$. C_p^0 : (A) 4.6×10^{-4} , (B) $3.2 \times 10^{-4} \text{ mol cm}^{-3}$. Supporting electrolyte: 0.2 M CF_3COONa +0.1 M $\text{CH}_3\text{COONa}/\text{CH}_3\text{COOH}$ (pH 5.5). Sampling times (ms) are given on each voltammogram.

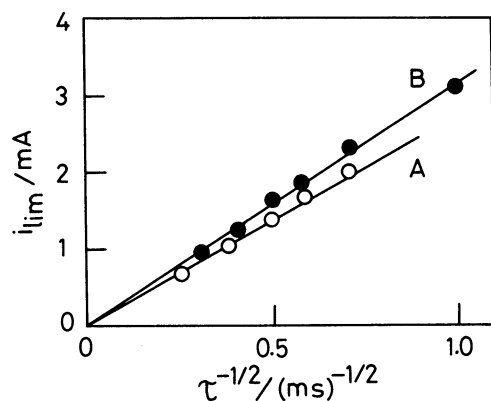


Fig. 6. Typical normal pulse voltammetric Cottrell plots of limiting current i_{lim} vs. $\tau^{-1/2}$ for the oxidation of (A) TAF^+ and (B) $[\text{Os}(\text{bpy})_3]^{2+}$ confined in the Nafion film on BPG electrodes. Experimental conditions are the same as in Fig. 5.

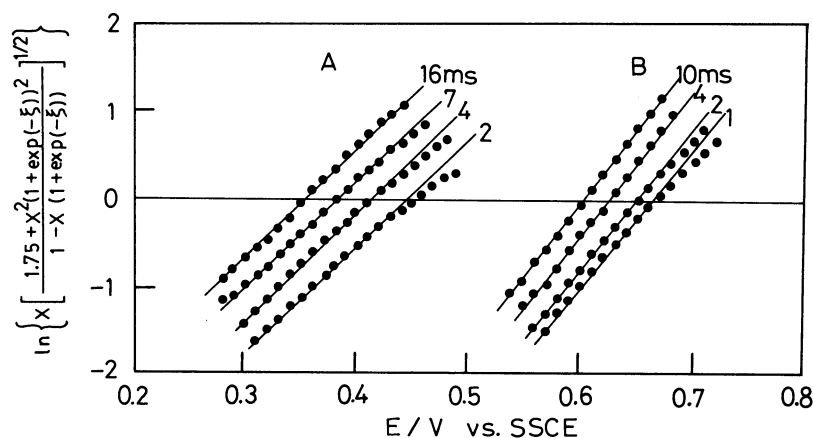


Fig. 7. Modified log plots of normal pulse voltammograms for the oxidation of (A) TFA^{+} and (B) $[\text{Os}(\text{bpy})_3]^{2+}$ complexes confined in the Nafion film. Sampling times (ms) are indicated on each straight line. Other experimental conditions are the same as in Fig. 5.

normal pulse voltammograms against the inverse square root of τ were found to be linear as expected for a diffusion-controlled limiting current (Fig. 6).^{2-6,8-14} Thus, the values of D_{app} were estimated from the slopes of the i_{lim} vs. $\tau^{-1/2}$ plots according to the normal pulse voltammetric Cottrell equation.^{2-6,8-14,31} Further, the kinetic parameters (i.e., standard rate constant (k°) and transfer coefficient (α)) of the heterogeneous electron-transfer reaction at the electrode/film interfaces could be estimated from an analysis of the rising part of the current-potential curves shown in Fig. 5, as described previously.^{2-6,8-14,29-31} The modified log plots for the normal pulse voltammograms of $\ln\{x[1.75+x^2(1+\exp(-\xi))^2]/\{1-x(1+\exp(-\xi))\}^{1/2}\}$ vs. E were found to be linear (Fig. 7) and the slopes of the straight lines were constant at the different τ 's in respective systems, where x is the ratio of the current at potential E to the anodic limiting diffusion current ($(i_d)_{\text{Cott}}$) expressed by the Cottrell equation and ξ is the dimensionless parameter expressed as $\{(nF/RT)(E-E_{1/2}^\circ)\}$ ($E_{1/2}^\circ$: the reversible half-wave potential, n : the number of electrons involved in the heterogeneous electron-transfer reaction, F : the Faraday constant, R : the gas constant, T : the absolute temperature). Thus, according to the previously described procedures,^{2-6,8-14,29-31} from the slopes of the straight lines and the intercepts of these lines with the axis, the values of k° and α were estimated. The values thus obtained of D_{app} , k° , and α are summarized in Fig. 9, together with those obtained by potential-step chronoamperometry (and chronocoulometry) and ac impedance measurements.

Alternating Current Impedance Measurements. In Fig. 8 are shown typical Cole-Cole plots (i.e., plots of the quadrature component of the ac impedance vs. its real component) for the redox reaction of the $[\text{Os}(\text{bpy})_3]^{2+/3+}$ and $\text{TAF}^{+/2+}$ couples confined in the

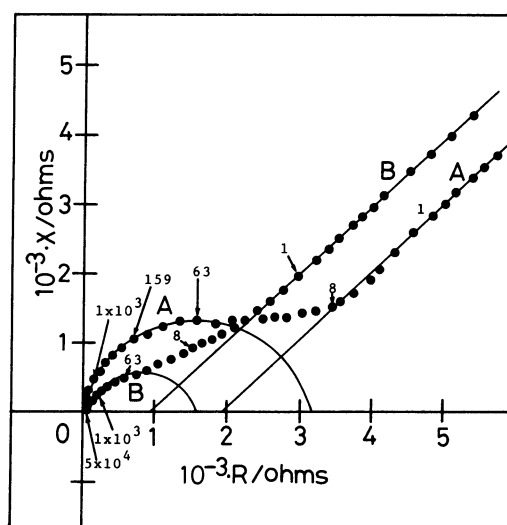


Fig. 8. Typical Cole-Cole plots for the redox reactions of (A) $\text{TAF}^{+/2+}$ and (B) $[\text{Os}(\text{bpy})_3]^{2+/3+}$ couples confined in the PFPC film on BPG electrodes in a 0.2 M CF_3COONa solution (pH 5.5) containing 0.1 M $\text{CH}_3\text{COONa}/\text{CH}_3\text{COOH}$ buffer. In both cases, the thicknesses of the PFPC films were 2.1×10^{-6} cm. C_p° : (A) 2.9×10^{-5} , (B) 1.7×10^{-4} mol cm^{-3} . The dc potentials were set at (A) 0.328 and (B) 0.586 V vs. SSCE which are formal redox potentials in cases A and B, respectively. The amplitude of an imposed ac voltage was 5.0 mV. X and R show the quadrature and real components of the ac impedance, respectively. The numbers on each plot represent frequency in units of Hz.

PFPC films on BPG electrodes in a 0.2 M CF_3COONa solution (pH 5.5). The data in Fig. 8 show the complex plane impedance plots for the redox reactions of these couples at each formal redox potential. These plots are considered to consist of the semicircular part and the straight line which corresponds to the Warburg diffusional impedance.^{32,34} It can be thus seen that the impedance loci of these

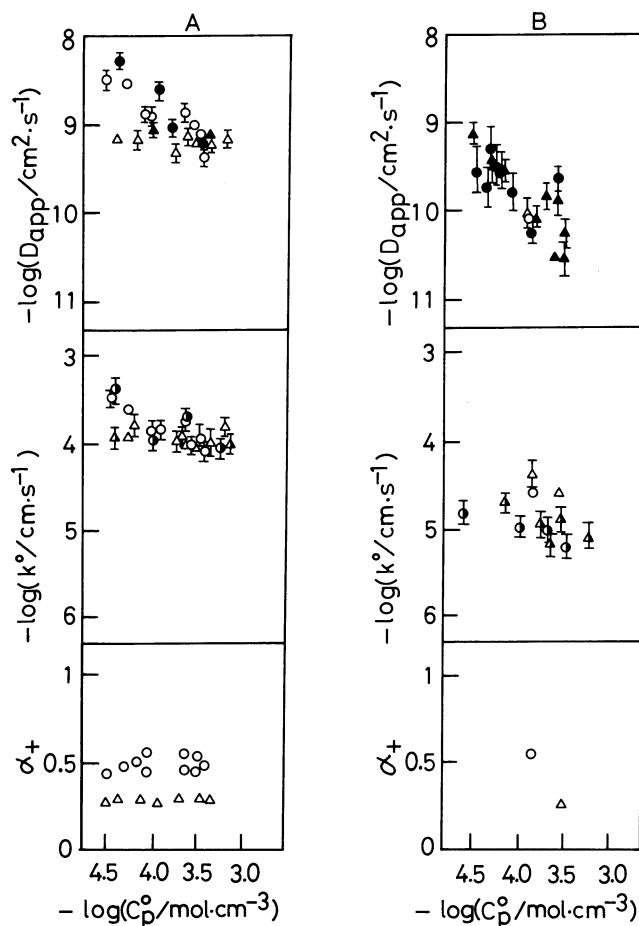


Fig. 9. Dependences of D_{app} , k° , and α_+ on C_p^0 . Coating films: (A) Nafion (Thickness: 4.3×10^{-5} cm). (B) PFPC (Thickness: 2.1×10^{-5} cm). Supporting electrolyte: 0.2 M CF_3COONa + 0.1 M $\text{CH}_3\text{COONa}/\text{CH}_3\text{COOH}$ (pH 5.5). (●, ○, △): $[\text{Os}(\text{bpy})_3]^{2+/3+}$, (▲, ▲, ▲): $\text{TAF}^{+/2+}$. Methods used for the measurements: (●, ▲) potential-step chronoamperometry and chronocoulometry; (○, △) ac impedance method; (○, △) normal pulse voltammetry.

plots correspond approximately to those expected for the electrochemical impedance represented by the well-known "Randles's equivalent circuit".³³⁾ Thus, the diameter of the semicircle enabled us to estimate the heterogeneous electron-transfer resistance and thus k° .^{32–34)} The k° values thus obtained for the redox reactions of the $\text{TAF}^{+/2+}$ and $[\text{Os}(\text{bpy})_3]^{2+/3+}$ couples confined in the Nafion or PFPC films at various C_p^0 values are shown in Fig. 9. The film resistances involving the solution resistance, obtained from the high-frequency intercept with the real axis, were in the range of ca. 20–50 Ω in both redox systems.

Temperature Dependences of $E^{\circ'}$, D_{app} , and k° . Figure 10 shows the temperature (T) dependences of the formal redox potentials ($E^{\circ'}$) for the $\text{TAF}^{+/2+}$ and $[\text{Os}(\text{bpy})_3]^{2+/3+}$ couples confined in the Nafion and PFPC films. The linear relationships between $E^{\circ'}$ and T were obtained and thus the reaction entropy

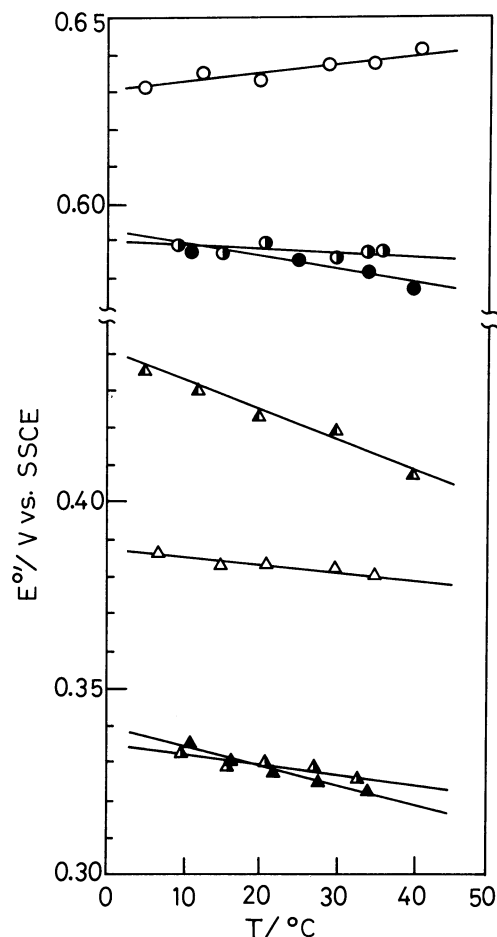


Fig. 10. Temperature dependences of the formal potentials ($E^{\circ'}$) of the $[\text{Os}(\text{bpy})_3]^{2+/3+}$ and $\text{TAF}^{+/2+}$ couples confined in the films. Confined redox couples: (○, ●, △) $[\text{Os}(\text{bpy})_3]^{2+/3+}$, (▲, ▲, ▲) $\text{TAF}^{+/2+}$. Coating films: (○, ▲, △) PFPC film (Thickness: 2.1×10^{-5} cm) (●, ●, ▲, ▲) Nafion film (Thickness: 4.3×10^{-5} cm). Supporting electrolyte: (▲) 0.2 M CF_3COONa (pH 1.0); (○, ●, ●, △, ▲, ▲) 0.2 M CF_3COONa + 0.1 M $\text{CH}_3\text{COONa}/\text{CH}_3\text{COOH}$ (pH 5.5). C_p^0 : (○) 1.4×10^{-4} ; (●) 6.6×10^{-5} ; (●) 2.6×10^{-5} ; (▲) 1.9×10^{-4} ; (△) 1.3×10^{-4} ; (▲) 6.6×10^{-4} ; (▲) 6.6×10^{-5} mol cm^{-3} .

differences (ΔS_{rc}^0) for these couples were estimated by using the equation:^{23, 25–28)}

$$\Delta S_{rc}^0 = S_{red}^0 - S_{ox}^0 = F(dE^{\circ'}/dT) \quad (1)$$

where S_{red}^0 and S_{ox}^0 are absolute ionic entropies of the reduced and oxidized halves of the redox couple and F is the Faraday constant. The temperature coefficient ($dE_i^{\circ'}/dT$) of the overall potential ($E_i^{\circ'}$) across the non-isothermal electrochemical cell consists of those of the Galvani metal-solution potential difference (ϕ_i^m), the potential difference across the thermal liquid junction within the 3 M NH_4Cl salt bridge (ϕ_{lij}) and the thermocouple potential difference between the hot and cold regions of the working electrode (ϕ_{tc}), which are expressed by $d\phi_i^m/dT$, $d\phi_{lij}/dT$, and $d\phi_{tc}/dT$, respectively.²³⁾ The value of $d\phi_{lij}/dT$ has been

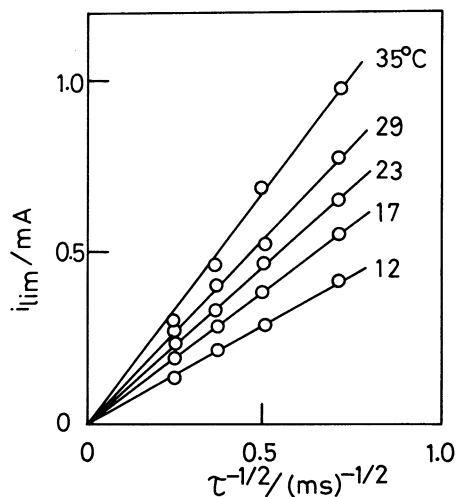


Fig. 11. Typical normal pulse voltammetric Cottrell plots of limiting current, i_{lim} , vs. (sampling time) $^{-1/2}$, $\tau^{-1/2}$, for the oxidation of the TAF $^{+}$ complex confined in the Nafion film on BPG electrodes at various temperatures. C_p^0 : 1.56×10^{-4} mol cm^{-3} . Film thickness: 4.3×10^{-5} cm. Other experimental conditions are the same as in Fig. 5.

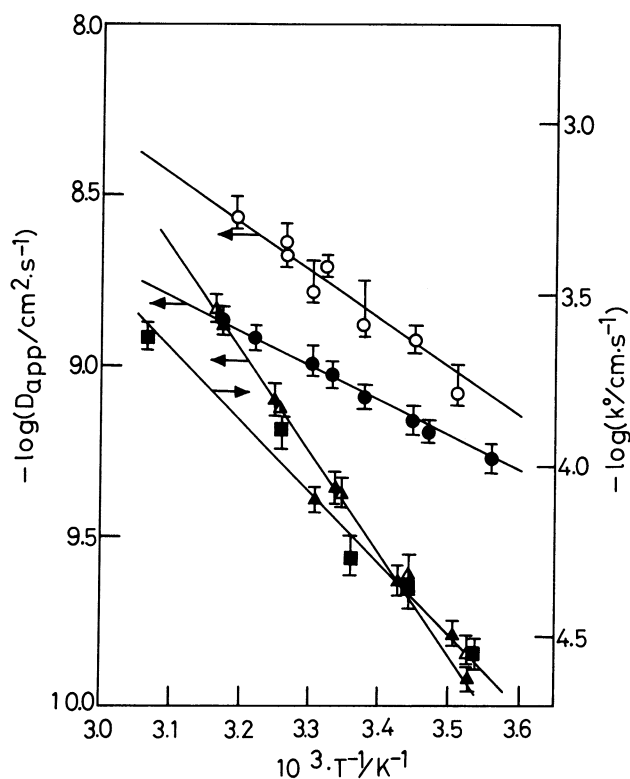


Fig. 12. Temperature dependences of D_{app} and k^0 for the $[\text{Os}(\text{bpy})_3]^{2+}$ and TAF $^{+}$ complexes confined in Nafion films. (O): $[\text{Os}(\text{bpy})_3]^{2+}$ (C_p^0 : 6.6×10^{-5} mol cm^{-3}), (\bullet): $[\text{Os}(\text{bpy})_3]^{2+}$ (C_p^0 : 2.6×10^{-4} mol cm^{-3}), (\blacktriangle , \blacksquare): TAF $^{+}$ (C_p^0 : 6.6×10^{-5} mol cm^{-3}), (\triangle): TAF $^{+}$ (C_p^0 : 6.6×10^{-4} mol cm^{-3}). Film thicknesses: 4.3×10^{-5} cm. Supporting electrolyte: 0.2 M $\text{CF}_3\text{COONa} + 0.1$ M $\text{CH}_3\text{COONa} / \text{CH}_3\text{COOH}$ (pH 5.5). Widths of error bars indicate uncertainties in the measurements of D_{app} and k^0 .

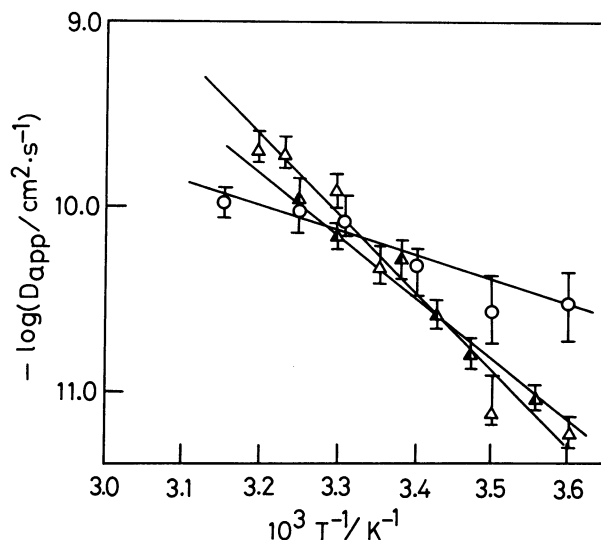


Fig. 13. Temperature dependences of D_{app} for the $[\text{Os}(\text{bpy})_3]^{2+}$ and TAF $^{+}$ complexes confined in PFPC films. (O): $[\text{Os}(\text{bpy})_3]^{2+}$ (C_p^0 : 1.4×10^{-4} mol cm^{-3}), (\blacktriangle): TAF $^{+}$ (C_p^0 : 1.9×10^{-4} mol cm^{-3}), (\triangle): TAF $^{+}$ (C_p^0 : 1.3×10^{-4} mol cm^{-3}). Film thickness: 2.1×10^{-5} cm. Supporting electrolyte: (\blacktriangle) 0.2 M CF_3COONa (pH 1.0); (O, \triangle): 0.2 M $\text{CF}_3\text{COONa} + \text{CH}_3\text{COONa} / \text{CH}_3\text{COOH}$ (pH 5.5). Widths of error bars indicate uncertainties in the measurements of D_{app} .

estimated to be less than $50 \mu\text{V K}^{-1}$.^{23,35} We have no data on the $d\phi_{\text{tc}}/dT$ for the BPG electrode, but it may be expected to be less than several tens of microvolts per degree from the $d\phi_{\text{tc}}/dT$ values for mercury and platinum which are 14 and $6 \mu\text{V K}^{-1}$, respectively.^{23,35} Thus we assumed that these temperature coefficients ($d\phi_{\text{tlj}}/dT$ and $d\phi_{\text{tc}}/dT$) can be negligible as compared with the experimental uncertainties ($\pm 2 \text{ cal mol}^{-1} \text{ K}^{-1}$ in ΔS_{tc}^0) in the present experiments.

In Fig. 11 is shown the typical dependence of the normal pulse voltammetric limiting current upon $\tau^{-1/2}$ for the oxidation of the TAF $^{+}$ confined in the Nafion film at different temperatures. From the slopes of such plots, the D_{app} 's at each temperature were obtained. Plots of the logarithm of D_{app} vs. T^{-1} were found to be linear over the temperature range 5–45 $^{\circ}\text{C}$, indicating that the behaviors are of the Arrhenius type (see Figs. 12 and 13). Thus, according to Eyring et al.,^{36,37} we can express the D_{app} as follows:

$$D_{\text{app}} = \lambda^2 \left(\frac{kT}{h} \right) \exp \left(\frac{\Delta S_{\text{diffusion}}^*}{R} \right) \exp \left(-\frac{\Delta H_{\text{diffusion}}^*}{RT} \right) \quad (2)$$

where $\Delta H_{\text{diffusion}}^*$ and $\Delta S_{\text{diffusion}}^*$ are the enthalpy and entropy, respectively, of activation for the homogeneous charge-transport process within the films, λ is the average distance between equilibrium positions in the process of diffusion, k is the Boltzmann constant, h is the Planck constant, and R is the gas constant. The values of λ have been unknown. Here, assuming that $\lambda=1$ and 10 \AA , the values of $\Delta S_{\text{diffusion}}^*$ are estimated (Different investigators^{37,38} have used values ranging

1 to 5 Å for λ). The obtained values of $\Delta H_{\text{diffusion}}^{\ddagger}$ and $\Delta S_{\text{diffusion}}^{\ddagger}$ are given in Table 2.

The temperature dependence of k° for the TAF⁺/2⁺ couple confined in the Nafion film is shown in Fig. 12, where the standard rate constants at the standard potential at each temperature are plotted against (temperature)⁻¹. According to Weaver et al.,^{21–23} who have recently demonstrated in detail the possibility and significance of such measurements using a non-isothermal cell (see Experimental Section) for simple electrode reactions, the “real” enthalpy and entropy of activation of the heterogeneous electron-transfer reaction ($(\Delta H_{\ddagger}^0)_{\text{real}}$ and $(\Delta S_{\ddagger}^0)_{\text{real}}$) were estimated to be $9.6 \pm 1.2 \text{ kcal mol}^{-1}$ and $-2 \pm 1 \text{ cal mol}^{-1} \text{ K}^{-1}$, respectively. In the estimation of $(\Delta S_{\ddagger}^0)_{\text{real}}$, the transmission coefficient (κ) introduced in order to account for possible non-adiabaticity of the electrode reaction was assumed to be unity.³⁹

Discussion

pH dependence of the Incorporation. From the data shown in Fig. 4, one can clearly see that the volume concentration (C_p^0) of the [Os(bpy)₃]²⁺ incorporated into the PFPC film increases from 1.4×10^{-5} to $3.2 \times 10^{-4} \text{ mol cm}^{-3}$ with increasing pH from 1 to 5.5, while C_p^0 of the incorporated TAF⁺ is almost independent of pH in the range of pH ca. 2–5.5 and is ca. $2 \times 10^{-4} \text{ mol cm}^{-3}$. This result for the [Os(bpy)₃]²⁺ complex is explained by the equilibrium competition of protons and [Os(bpy)₃]²⁺ ions for counterionic sites within the PFPC film. That is, at pH values as low as 1, protons compete quite successfully with [Os(bpy)₃]²⁺ ions for counterionic sites within the PFPC, and with increasing pH [Os(bpy)₃]²⁺ ions become dominantly trapped. The shape of the plot for the [Os(bpy)₃]²⁺ resembles that of a typical pH titration curve. Thus, the effective pK_a of the carboxylic acid group in the PFPC is estimated to be ca. 2.9 from the pH at which the incorporation reaches one-half of its maximum value. This value is different from that (2.2) obtained from the incorporation experiments of [Ru(NH₃)₆]³⁺ into the PFPC¹⁶ and also from the pK_a of 1.9 measured directly for a similar perfluoro carboxylate polyelectrolyte.⁴⁰ As generally well-known, the effective pK_a of polyelectrolytes varies with the degree of protonation and with the ionic strength.⁴¹ These are considered as main reasons for the different effective pK_a 's.

On the other hand, the situation for the TAF⁺ complex seems to be different from that for the above-mentioned [Os(bpy)₃]²⁺ complex. The incorporation of TAF⁺ complex changes slightly with pH, especially at pH < ca. 2. In this case, the effective pK_a , which is estimated from the C_p^0 vs. pH curve by the same procedure as that used for the pK_a determination of the PFPC polyelectrolyte from the [Os(bpy)₃]²⁺ incorporation experiments, is ca. 1, being clearly different from

that obtained from the [Os(bpy)₃]²⁺ incorporation experiments. The amount of the incorporation of the TAF⁺ complex is comparable to the maximum value for the [Os(bpy)₃]²⁺ complex, as seen from the C_p^0 values for [Os(bpy)₃]²⁺ and TAF⁺ at pH 5.5.

These different pH-dependences of the incorporation of [Os(bpy)₃]²⁺ and TAF⁺ complexes into the PFPC film should be noted, because this result can be considered to suggest different interactions (between the complexes and the PFPC film) by which these complexes are incorporated into the film and confined in it. In the case of the Nafion (or poly(*p*-styrenesulfonate)) film, such a pH-dependence of the incorporation of the same complexes was not observed in the examined range of pH 1 to 5.5.⁶¹ Thus, the observed pH-dependences of the incorporation are peculiar to the PFPC film. The feature to be noted on the basis of the above-mentioned incorporation experiments is that the morphology of the PFPC film changes from the non-ionic polymer film to the anionic polyelectrolyte film with cation-exchange properties with increasing pH from ca. 1 to 5.5. In the case of the [Os(bpy)₃]²⁺ complex, the incorporation can be considered to be mainly due to “electrostatic interactions”^{2–8, 11, 13, 19, 41–48, 52} between anionic carboxylic sites in the PFPC and cationic [Os(bpy)₃]²⁺ complexes. The C_p^0 values were about 1.4×10^{-5} and $2.5 \times 10^{-4} \text{ mol cm}^{-3}$ at pH 1 and 5.5, respectively, where the PFPC films are in the nonionic and anionic states, respectively. Thus, the difference between the C_p^0 values at pH 1 and 5.5 is considered to approximately correspond to the incorporation amount of [Os(bpy)₃]²⁺ by electrostatic interactions. In addition, the C_p^0 value of $1.4 \times 10^{-5} \text{ mol cm}^{-3}$ at pH 1 may be regarded as the amount of the [Os(bpy)₃]²⁺ complex incorporated into the film by specific interactions other than such electrostatic interactions, for example, “hydrophobic interactions”^{16, 17, 42} between the large fluorocarbon component of the polyelectrolyte coating and [Os(bpy)₃]²⁺ complexes. On the other hand, in the case of the TAF⁺ complex, the situation seems different. Unlike the [Os(bpy)₃]²⁺ complex, there may be probably a minor contribution of electrostatic interactions to the incorporation. This is deducible from the fact that C_p^0 scarcely depends on pH. In this case, the incorporation seems to be mainly due to “hydrophobic interaction”.^{16, 17, 42}

Apparent Diffusion Coefficients for Diffusion-Like Charge Transport within Nafion and PFPC Films. The data shown in Fig. 9 demonstrate the dependences of D_{app} on the redox complex confined in the film, its concentration (C_p^0) and the film confining it. For example, when C_p^0 was increased from 3.2×10^{-5} to $3.2 \times 10^{-4} \text{ mol cm}^{-3}$, D_{app} decreased from 4.7×10^{-9} to $4.5 \times 10^{-10} \text{ cm}^2 \text{ s}^{-1}$ in the case of the Nafion–[Os(bpy)₃]²⁺ system, while in the case of the Nafion–TAF⁺ system D_{app} was found to slightly decrease. For the PFPC coatings, the dependences of D_{app} on C_p^0 were

almost the same in both $[\text{Os}(\text{bpy})_3]^{2+}$ and TAF^+ systems: D_{app} decreased from 8.3×10^{-10} to $5.1 \times 10^{-11} \text{ cm}^2 \text{ s}^{-1}$ with an increase in C_p^0 from 3.2×10^{-5} to $3.2 \times 10^{-4} \text{ mol cm}^{-3}$. These observed decreases of D_{app} 's with increasing C_p^0 may be understood by the same idea as that used to explain the concentration dependences of D_{app} 's found in the other previously reported redox polymer films:^{2-14,42,46-48} These decreases are considered to be attributed to the effects of "electrostatic (or hydrophilic) cross linking"^{2-8,11,13,16,17,19,41-48,52} of the films by the electrostatic (or hydrophilic) interactions between the redox ions and the polyelectrolytes containing them (as mentioned above) and/or of "single-file diffusion",^{42,43,49} An increase of the electrostatic cross linking with increasing C_p^0 causes a decrease in the diffusion rate of redox ion itself as well as decreases in the rates of the charge-compensating counterion motion which is necessarily coupled to electron transfer, the motion of solvent and/or the segmental motion of the polymeric chain. Also, the diffusing species which must move between more or less fixed sites within a polymeric matrix are considered to have their rate of motion limited by the decreasing availability of sites as C_p^0 of the diffusing species increases. These result in the decrease of the overall rate of the charge transport with an increase in C_p^0 and thus the decreased D_{app} 's are observed. It is also apparent from Fig. 9 that at a given C_p^0 the values of D_{app} for the Nafion-TAF⁺ and $[\text{Os}(\text{bpy})_3]^{2+}$ systems are larger than those for the PFPC-TAF⁺ and $[\text{Os}(\text{bpy})_3]^{2+}$ systems. For example, at $C_p^0 = 1.0 \times 10^{-4} \text{ mol cm}^{-3}$, the values of D_{app} are 1.5×10^{-9} and $1.8 \times 10^{-10} \text{ cm}^2 \text{ s}^{-1}$ for the Nafion- $[\text{Os}(\text{bpy})_3]^{2+}$ and PFPC- $[\text{Os}(\text{bpy})_3]^{2+}$ systems, respectively, and those are 6.2×10^{-10} and $1.0 \times 10^{-10} \text{ cm}^2 \text{ s}^{-1}$ for the Nafion-TAF⁺ and PFPC-TAF⁺ systems, respectively.

The Dependence of D_{app} on pH is of interest in connection with the pH dependence of the incorporation of the $[\text{Os}(\text{bpy})_3]^{2+}$ and TAF^+ complexes (Fig. 4). For the $[\text{Os}(\text{bpy})_3]^{2+}$ system, the D_{app} decreased with increasing pH. This means that the decrease of D_{app} is owing to the increase of C_p^0 , because C_p^0 increases with increasing pH as mentioned above. When pH was increased from 1 to 5.5, C_p^0 increased from 1.4×10^{-5} to

$3.2 \times 10^{-4} \text{ mol cm}^{-3}$ and thus D_{app} decreased from 1.4×10^{-9} to $2.1 \times 10^{-10} \text{ cm}^2 \text{ s}^{-1}$. For the TAF⁺ system, on the other hand, D_{app} 's were almost independent of pH and were ca. $1.2 \times 10^{-10} \text{ cm}^2 \text{ s}^{-1}$. Such a pH-independence of D_{app} can be expected, because C_p^0 rarely varies with pH in the examined range of pH.

Kinetic Parameters of Heterogeneous Electron-Transfer Reactions at Electrode/Film Interfaces.

The k^0 values for a given system, estimated by normal pulse voltammetry and ac impedance method, were almost the same within experimental error as shown in Fig. 9.⁵⁵ It appears that k^0 depends, though slightly, on C_p^0 . For example, when C_p^0 was increased from 3.2×10^{-5} to $3.2 \times 10^{-4} \text{ mol cm}^{-3}$, k^0 decreased from ca. 3×10^{-4} to $7 \times 10^{-5} \text{ cm s}^{-1}$ in the case of the Nafion- $[\text{Os}(\text{bpy})_3]^{2+}$ system and from ca. 2×10^{-5} to $7 \times 10^{-6} \text{ cm s}^{-1}$ in the case of the PFPC- $[\text{Os}(\text{bpy})_3]^{2+}$ and TAF⁺ systems. In the case of the Nafion-TAF⁺ system, k^0 seemed almost independent of C_p^0 . Further, the values of k^0 for the Nafion- $[\text{Os}(\text{bpy})_3]^{2+}$ and TAF⁺ systems are larger than those for the PFPC- $[\text{Os}(\text{bpy})_3]^{2+}$ and TAF⁺ systems, for example, at $C_p^0 = 1.0 \times 10^{-4} \text{ mol cm}^{-3}$ the k^0 values (ca. $1 \times 10^{-4} \text{ cm s}^{-1}$) for the former systems are about one order of the magnitude larger than those for the latter systems. The transfer coefficients were almost independent of the polymer films: The anodic transfer coefficients (α_+) for the oxidation of the $[\text{Os}(\text{bpy})_3]^{2+}$ complex confined in the Nafion and PFPC films are 0.48 and 0.51, respectively, and those for the oxidation of the TAF⁺ complex confined in the Nafion and PFPC films are 0.29 and 0.24, respectively.

Formal Potentials and Reaction Entropies for the $[\text{Os}(\text{bpy})_3]^{2+/3+}$ and $\text{TAF}^{+/2+}$ Couples Confined in Films. The formal potentials (E^0) of the $[\text{Os}(\text{bpy})_3]^{2+/3+}$ and $\text{TAF}^{+/2+}$ couples largely varied with the films confining them (see Table 1), indicating that the relative equilibrium binding constants for two halves of a redox couple are not determined solely by the magnitudes of their positive charges. In the PFPC film, the less highly charged (i.e., reduced) form of each couple is stabilized larger, while in the Nafion film the more highly charged (i.e., oxidized) form is stabilized larger. As a result, the E^0 values for the

Table 1. Formal Redox Potentials and Reaction Entropies for the $[\text{Os}(\text{bpy})_3]^{2+/3+}$ and $\text{TAF}^{+/2+}$ Couples Confined in Nafion and PEPC Films

Film	Redox species	$C_p^0/\text{mol cm}^{-3}$ ^{a)}	$E^0/\text{V vs. SSCE}$ ^{b)}	$\Delta S_r^\circ/\text{cal mol}^{-1} \text{ K}^{-1}$ ^{c)}
Nafion	$[\text{Os}(\text{bpy})_3]^{2+/3+}$ ^{d)}	6.6×10^{-5}	0.587 ± 0.003	-8 ± 2
Nafion	$[\text{Os}(\text{bpy})_3]^{2+/3+}$ ^{d)}	2.6×10^{-4}	0.584 ± 0.003	-9 ± 2
Nafion	$\text{TAF}^{+/2+}$ ^{d)}	6.0×10^{-5}	0.326 ± 0.003	-11 ± 2
Nafion	$\text{TAF}^{+/2+}$ ^{d)}	6.0×10^{-4}	0.328 ± 0.003	-7 ± 2
PFPC	$[\text{Os}(\text{bpy})_3]^{2+/3+}$ ^{d)}	1.4×10^{-4}	0.637 ± 0.003	5 ± 2
PFPC	$\text{TAF}^{+/2+}$ ^{d)}	1.9×10^{-4}	0.385 ± 0.003	-5 ± 2
PFPC	$\text{TAF}^{+/2+}$ ^{e)}	1.3×10^{-4}	0.419 ± 0.003	-19 ± 2

a) Concentration of redox species confined in films. b) Formal redox potentials for the redox couples confined in films at 298 K. c) Reaction entropies for the redox couples confined in films (see text). d) Supporting electrolyte: 0.2 M $\text{CF}_3\text{COONa} + 0.1 \text{ M CH}_3\text{COONa}/\text{CH}_3\text{COOH}$ (pH 5.5). e) Supporting electrolyte: 0.2 M CF_3COONa (pH 1.0).

$[\text{Os}(\text{bpy})_3]^{2+/3+}$ and $\text{TAF}^{+/2+}$ couples confined in the PFPC film are more positive than those of these couples confined in the Nafion film. Further, in the PFPC film, the reduced form of the $\text{TAF}^{+/2+}$ couple is more stabilized at pH 1.0 than at pH 5.5. Thus, the values of E^0 for these two couples indicate the more dominance of hydrophobic interactions for the $\text{TAF}^{+/2+}$ couple, compared with the $[\text{Os}(\text{bpy})_3]^{2+/3+}$ couple where hydrophilic interactions are more dominant. This is also supported by the data of the incorporation of TAF^{+} and $[\text{Os}(\text{bpy})_3]^{2+}$ into the PFPC film (mentioned in the previous section). The present data seem to suggest that the hydrophobicity of the $\text{TAF}^{+/2+}$ couple is larger than that of the $[\text{Os}(\text{bpy})_3]^{2+/3+}$ couple, in contrast to the previously reported results.¹⁶⁾

The negative reaction entropy differences (ΔS_{rc}^0) were obtained except for the PFPC- $[\text{Os}(\text{bpy})_3]^{2+}$ system. These negative ΔS_{rc}^0 values may suggest that the net solvent ordering in the vicinity of the redox species is less extensive in the oxidized state than in the reduced state in qualitative disagreement with the expectations from an electrostatic treatment (e.g., by the Born model⁵⁰⁾). This is considered as a result of the hydrophobic interactions between the redox species and the surroundings (in the swollen Nafion and PFPC films) that are enhanced in the reduced state, leading to increased solvent ordering and a decrease in entropy compared with that for the oxidized state. Large negative values of ΔS_{rc}^0 have been recently reported for the $[\text{Ru}(\text{NH}_3)_6]^{3+/2+}$ couple confined in the PFPC film on graphite electrodes¹⁶⁾ and the ferricinium-ferrocene couple attached to platinum electrodes.²⁸⁾ Negative values of ΔS_{rc}^0 have also been observed for the bulk-solution blue copper

proteins⁵³⁾ and ferricinium-ferrocene couple.⁵⁴⁾

On the other hand, the positive ΔS_{rc}^0 value obtained for the PFPC- $[\text{Os}(\text{bpy})_3]^{2+}$ system may be explained as follows: The increased polarization of water molecules adjacent to the aromatic rings of $[\text{Os}(\text{bpy})_3]^{2+}$ ions occurs in the higher oxidation state and, as a result, the positive ΔS_{rc}^0 is obtained.

Activation Parameters for Homogeneous Charge-Transport Process and Heterogeneous Electron-Transfer Reaction. From the data in Table 2, some thermodynamic aspects on the homogeneous charge-transport process within the Nafion and PFPC films containing $[\text{Os}(\text{bpy})_3]^{2+}$ or TAF^{+} can be drawn as mentioned below. For a given film, the values of both $\Delta H_{\text{diffusion}}^*$ and $\Delta S_{\text{diffusion}}^*$ for the TAF^{+} complex are larger than those for the $[\text{Os}(\text{bpy})_3]^{2+}$ complex.⁶⁰⁾ The values of D_{app} for the former complex are smaller than those for the latter complex. Thus, the charge-transport processes within the films containing TAF^{+} are more favorable entropically and more unfavorable enthalpically, compared with those within the films containing $[\text{Os}(\text{bpy})_3]^{2+}$ and as a whole the smaller values of D_{app} for the TAF^{+} complex are due to the larger $\Delta H_{\text{diffusion}}^*$. In the case of the PFPC- TAF^{+} system, the D_{app} 's obtained at pH 1.0 and pH 5.5 are almost the same. This results from the mutual compensation of the $\Delta H_{\text{diffusion}}^*$ and $\Delta S_{\text{diffusion}}^*$ terms, although the absolute values of $\Delta H_{\text{diffusion}}^*$ and $\Delta S_{\text{diffusion}}^*$ are largely different at these both pH's. As mentioned in the previous section, the incorporation of the TAF^{+} complex into the PFPC film is due to mainly hydrophobic interactions, while in the case of the Nafion and PFPC- $[\text{Os}(\text{bpy})_3]^{2+}$ systems an electrostatic interaction is the main force for the incorporation of the $[\text{Os}(\text{bpy})_3]^{2+}$ (and $[\text{Os}(\text{bpy})_3]^{3+}$) complexes

Table 2. Activation Parameters for Homogeneous Charge Transport in Nafion and PFPC Films

Film	Redox species	$C_p^0/\text{mol cm}^{-3\text{a)}$	$D_{\text{app}}/\text{cm}^2 \text{s}^{-1\text{b)}$
Nafion	$[\text{Os}(\text{bpy})_3]^{2+/3+\text{d)}$	6.6×10^{-5}	21×10^{-10}
Nafion	$[\text{Os}(\text{bpy})_3]^{2+/3+\text{d)}$	2.6×10^{-4}	11×10^{-10}
Nafion	$\text{TAF}^{+/2+\text{e)}$	6.0×10^{-5}	8.0×10^{-10}
Nafion	$\text{TAF}^{+/2+\text{e)}$	6.0×10^{-4}	7.9×10^{-10}
PFPC	$[\text{Os}(\text{bpy})_3]^{2+/3+\text{d)}$	1.7×10^{-4}	7.9×10^{-10}
PFPC	$\text{TAF}^{+/2+\text{e)}$	1.9×10^{-4}	0.9×10^{-10}
PFPC	$\text{TAF}^{+/2+\text{h)}$	1.3×10^{-4}	1.7×10^{-10}

Film	$\Delta H_{\text{diffusion}}^*/\text{kcal mol}^{-1\text{c)}$	$\Delta S_{\text{diffusion}}^*/\text{cal mol}^{-1} \text{K}^{-1\text{d)}$
Nafion	6.5 ± 0.5	$-13 \pm 2^{\text{e)}$ $-3 \pm 2^{\text{f)}$
Nafion	4.9 ± 0.6	$-23 \pm 2^{\text{e)}$ $-13 \pm 2^{\text{f)}$
Nafion	10 ± 1.0	$7 \pm 2^{\text{e)}$ $16 \pm 2^{\text{f)}$
Nafion	10 ± 1.0	$7 \pm 2^{\text{e)}$ $16 \pm 2^{\text{f)}$
PFPC	6.7 ± 0.6	$-19 \pm 2^{\text{e)}$ $-10 \pm 2^{\text{f)}$
PFPC	12 ± 1.2	$-2 \pm 2^{\text{e)}$ $7 \pm 2^{\text{f)}$
PFPC	18 ± 3.0	$7 \pm 3^{\text{e)}$ $16 \pm 3^{\text{f)}$

a) Concentration of redox species confined in films. b) Values at 298 K. c) Activation enthalpies for homogeneous charge-transport in films. d) Activation entropies for homogeneous charge-transport in films. e) Calculated from Eq. 2 assuming $\lambda = 10 \text{ \AA}$ at 298 K. f) Calculated from Eq. 2 assuming $\lambda = 1 \text{ \AA}$ at 298 K. g) Supporting electrolyte: 0.2 M $\text{CF}_3\text{COONa} + 0.1 \text{ M } \text{CH}_3\text{COONa}/\text{CH}_3\text{COOH}$ (pH 5.5). h) Supporting electrolyte: 0.2 M CF_3COONa (pH 1.0).

into these films. From the combination of these facts and the data in Table 2, it may be concluded that in the case of the incorporation by hydrophobic interactions both $\Delta H_{\text{diffusion}}^{\ddagger}$ and $\Delta S_{\text{diffusion}}^{\ddagger}$ are larger than those in the case of the incorporation by electrostatic interactions. In the latter case, an increase in C_p^0 causes a decrease in D_{app} , and in this case the $\Delta S_{\text{diffusion}}^{\ddagger}$ values are negative and decrease with increasing C_p^0 . Similar results have been previously obtained for protonated poly(4-vinylpyridine) film- $[\text{W}(\text{CN})_8]^{4-}$ and $[\text{IrCl}_6]^{3-}$ systems.⁴⁾ Electrostatic cross linking and single-file diffusion effects seem to mainly be reflected as "negative" $\Delta S_{\text{diffusion}}^{\ddagger}$ values. In the case of the Nafion-TAF⁺ system, the D_{app} values are almost independent of C_p^0 and the $\Delta H_{\text{diffusion}}^{\ddagger}$ and $\Delta S_{\text{diffusion}}^{\ddagger}$ values are also independent of C_p^0 .

The "real" entropy ($(\Delta S_{\ddagger}^0)_{\text{real}}^{21-23}$) of activation for the heterogeneous electron-transfer reaction of the TAF^{+/2+} couple confined in the Nafion film is negative (close to zero) ($-2 \pm 1 \text{ cal mol}^{-1} \text{ K}^{-1}$). This fact seems to be remarkable,⁵¹⁾ although at the present stage we have no satisfactory explanation for this. In the estimation of $(\Delta S_{\ddagger}^0)_{\text{real}}$, the transmission coefficient (κ)³⁹⁾ was assumed as unity. Thus, it may be also probable that if $(\Delta S_{\ddagger}^0)_{\text{real}}$ has a "normal" positive value, κ should be smaller than 1 and thus the heterogeneous electron-transfer reaction would be nonadiabatic.^{39,51)}

The present work was partially supported by Grant-in-Aid for Scientific Research No. 62470071, for N. Oyama, from the Ministry of Education, Science and Culture.

References

- 1) See, for example, (a) R. W. Murray, "Electroanal. Chem.," ed by A. J. Bard, Marcel Dekker Inc., (1984), Vol. 13, p. 191. (b) A. R. Hillman, "Electrochemical Science & Technology 1," ed by R. G. Linford, Elsevier Applied Science Inc., (1987), p. 103.
- 2) N. Oyama, T. Ohsaka, M. Kaneko, K. Sato, and H. Matsuda, *J. Am. Chem. Soc.*, **105**, 6003 (1983).
- 3) K. Sato, S. Yamaguchi, H. Matsuda, T. Ohsaka, and N. Oyama, *Bull. Chem. Soc. Jpn.*, **56**, 2004 (1983).
- 4) N. Oyama, T. Ohsaka, and T. Ushirogouchi, *J. Phys. Chem.*, **88**, 5274 (1984).
- 5) T. Ohsaka, H. Yamamoto, M. Kaneko, A. Yamada, M. Nakamura, S. Nakamura, and N. Oyama, *Bull. Chem. Soc. Jpn.*, **57**, 1844 (1984).
- 6) T. Ohsaka, K. Sato, H. Matsuda, and N. Oyama, *J. Electrochem. Soc.*, **132**, 1871 (1985).
- 7) T. Ohsaka, T. Ushirogouchi, and N. Oyama, *Bull. Chem. Soc. Jpn.*, **58**, 3252 (1985).
- 8) N. Oyama, T. Ohsaka, and T. Shimizu, *Anal. Chem.*, **57**, 1526 (1985).
- 9) N. Oyama, T. Ohsaka, H. Yamamoto, and M. Kaneko, *J. Phys. Chem.*, **90**, 3850 (1986).
- 10) N. Oyama, K. Hirabayashi, and T. Ohsaka, *Bull. Chem. Soc. Jpn.*, **59**, 2071 (1986).
- 11) N. Oyama, T. Ohsaka, and M. Nakanishi, *J. Macromol. Sci.-Chem.*, **A24**, 375 (1987).
- 12) T. Ohsaka, K. Chiba, and N. Oyama, *Nippon Kagaku Kaishi*, **1986**, 457.
- 13) T. Ohsaka, T. Okajima, and N. Oyama, *J. Electroanal. Chem.*, **215**, 191 (1986).
- 14) K. Chiba, T. Ohsaka, and N. Oyama, *J. Electroanal. Chem.*, **217**, 239 (1987).
- 15) H. S. White, J. Leddy, and A. J. Bard, *J. Am. Chem. Soc.*, **104**, 4811 (1982).
- 16) Y.-M. Tsou and F. C. Anson, *J. Electrochem. Soc.*, **131**, 595 (1984).
- 17) N. Oyama, T. Ohsaka, K. Sato, and H. Yamamoto, *Anal. Chem.*, **55**, 1429 (1983).
- 18) C. Creutz, M. Chou, T. L. Netzel, M. Okumura, and N. J. Sutin, *J. Am. Chem. Soc.*, **102**, 1309 (1980).
- 19) N. Oyama and F. C. Anson, *Anal. Chem.*, **52**, 1192 (1980).
- 20) I. Rubinstein and A. J. Bard, *J. Am. Chem. Soc.*, **103**, 5007 (1981).
- 21) M. J. Weaver, *J. Phys. Chem.*, **83**, 1748 (1979).
- 22) M. J. Weaver, *J. Phys. Chem.*, **80**, 2645 (1976).
- 23) E. L. Yee, R. J. Cave, Y. L. Guyer, P. C. Tyme, and M. J. Weaver, *J. Am. Chem. Soc.*, **101**, 1131 (1979).
- 24) J. T. Hupp and M. J. Weaver, *J. Electroanal. Chem.*, **145**, 43 (1983).
- 25) M. J. Weaver and S. M. Nettles, *Inorg. Chem.*, **19**, 1641 (1980).
- 26) N. Sutin, M. J. Weaver, and E. L. Yee, *Inorg. Chem.*, **19**, 1096 (1980).
- 27) J. T. Hupp and M. J. Weaver, *Inorg. Chem.*, **23**, 3639 (1984).
- 28) J. T. Hupp and M. J. Weaver, *J. Electrochem. Soc.*, **131**, 619 (1984).
- 29) T. Ohsaka, N. Oyama, S. Yamaguchi, and H. Matsuda, *Bull. Chem. Soc. Jpn.*, **54**, 2475 (1981).
- 30) S. Yamaguchi, H. Matsuda, T. Ohsaka, and N. Oyama, *Bull. Chem. Soc. Jpn.*, **56**, 2952 (1983).
- 31) H. Matsuda, *Bull. Chem. Soc. Jpn.*, **53**, 3439 (1980).
- 32) M. Sluyters-Rehbach and J. H. Sluyters, "Electroanalytical Chemistry," Vol. 4, ed by A. J. Bard, Marcel Dekker, New York (1970), p. 1.
- 33) J. E. B. Randles, *Discuss. Faraday Soc.*, **1**, 11 (1947).
- 34) A. J. Bard and L. R. Faulkner, "Electrochemical Methods, Fundamentals and Applications," Wiley, New York (1980), p. 316.
- 35) J. N. Agar, *Adv. Electrochem. Electrochem. Eng.*, **3**, 31 (1963).
- 36) H. Eyring, *J. Chem. Phys.*, **4**, 283 (1936).
- 37) S. Glasstone, K. J. Laidler, and H. Eyring, "The Theory of Rate Processes," McGraw Hill, New York (1941), p. 525.
- 38) M. M. Berg, K. Ahmad, I. Altaf, and M. Arshad, *J. Mem. Sci.*, **9**, 303 (1981) and references therein.
- 39) R. A. Marcus, *J. Chem. Phys.*, **43**, 679 (1965) and references therein.
- 40) Z. Twardowski, H. L. Yeager, and B. O'Dell, *J. Electrochem. Soc.*, **129**, 328 (1982).
- 41) H. Zumbunnen and F. C. Anson, *J. Electroanal. Chem.*, **152**, 111 (1983).
- 42) D. A. Buttry and F. C. Anson, *J. Am. Chem. Soc.*, **105**, 685 (1983).
- 43) Y.-M. Tsou and F. C. Anson, *J. Phys. Chem.*, **89**, 3818

(1985).

44) J. Facci and R. W. Murray, *J. Electroanal. Chem.*, **124**, 339 (1981).

45) K.-N. Kuo and R. W. Murray, *J. Electroanal. Chem.*, **131**, 37 (1982).

46) N. Oyama and F. C. Anson, *J. Electrochem. Soc.*, **127**, 640 (1980).

47) N. Oyama, T. Shimomura, K. Shigehara, and F. C. Anson, *J. Electroanal. Chem.*, **112**, 271 (1980).

48) F. C. Anson, T. Ohsaka, and J. M. Saveant, *J. Phys. Chem.*, **87**, 640 (1983).

49) K. Heckmann, "Biomembranes," ed by A. L. Manson, Plenum Press, New York (1972), Vol. 3, p. 127.

50) R. M. Noyes, *J. Am. Chem. Soc.*, **84**, 513 (1962).

51) T. Ohsaka, H. Yamamoto, and N. Oyama, *J. Phys. Chem.*, **91**, 3775 (1987).

52) N. Oyama, T. Ohsaka, and T. Okajima, *Anal. Chem.*, **58**, 979 (1986).

53) N. Sailasuta, F. C. Anson, and H. B. Gray, *J. Am. Chem. Soc.*, **101**, 455 (1979).

54) E. L. Yee and M. J. Weaver, *Inorg. Chem.*, **19**, 1077 (1980).

55) The conventional positive feedback techniques^{56,57} were used to compensate the resistances associated with the polymer coatings as much as possible. That is, a normal pulse voltammetric experiment was carried out in a potential region preceding the wave corresponding to the oxidation of $[\text{Os}(\text{bpy})_3]^{2+}$ (or TAF^+) confined in Nafion (or PFPC) films, where the current was due almost entirely to double-layer charging. The extent of compensation was increased until the onset of oscillation and then it was

reduced slightly. Using these techniques, the residual uncompensated resistance can be, though not completely, decreased below typically ca. several ohms.^{58,59} By comparing the uncompensated resistance with the heterogeneous electron-transfer resistances which were in the range of a few hundreds to thousands (in ohm) (as typically shown in Fig. 8), we conclude that uncompensated resistance is not a major contributor to error in the measurement.

56) A. J. Bard and L. R. Faulkner, "Electrochemical Methods, Fundamentals and Applications," Wiley, New York (1980), Chap. 13.

57) D. T. Sawyer and J. L. Robert, "Experimental Electrochemistry for Chemists," Wiley, New York (1974), Chap. 5.

58) P. E. Whitson, H. W. VandenBorn, and D. H. Evans, *Anal. Chem.*, **45**, 1298 (1973).

59) T. W. Ronsanske and D. H. Evans, *J. Electroanal. Chem.*, **72**, 277 (1976).

60) The differences between $\Delta S_{\text{diffusion}}^*$ values obtained for the $[\text{Os}(\text{bpy})_3]^{2+}$ and TAF^+ complexes confined in Nafion films were 29–30 cal mol⁻¹ K⁻¹ and those obtained for the same complexes confined in PFPC films were 17–26 cal mol⁻¹ K⁻¹ (Table 2). These differences in $\Delta S_{\text{diffusion}}^*$ values are fairly larger than those (4–5 cal mol⁻¹ K⁻¹) between the $\Delta S_{\text{diffusion}}^*$ values estimated using λ values ranging 1 to 5 Å^{37,38} which have usually been used in a quantitative analysis of the process of diffusion.

61) The sulfonate ion-exchange sites of Nafion perfluoro-sulfonate and poly(*p*-styrenesulfonate) films show strong acid behavior ($\text{p}K_a < 1$).⁴⁰